Molecular Biology of the Cell
Vol. 18, 2216–2225, June 2007

Mitotic Chromosome Biorientation in Fission Yeast Is Enhanced by Dynein and a Minus-end–directed, Kinesin-like Protein[D] [V]

Ekaterina L. Grishchuk,*† Ilia S. Spiridonov,*‡ and J. Richard McIntosh*

*Molecular, Cellular, and Developmental Biology Department, University of Colorado at Boulder, Boulder, CO 80309; †Institute of General Pathology and Pathophysiology, Moscow 125315, Russia; and ‡National Research Center for Hematology, Moscow 125167, Russia

Submitted November 6, 2006; Revised February 27, 2007; Accepted March 22, 2007
Monitoring Editor: Kerry Bloom

Chromosome biorientation, the attachment of sister kinetochores to sister spindle poles, is vitally important for accurate chromosome segregation. We have studied this process by following the congression of pole-proximal kinetochores and their subsequent anaphase segregation in fission yeast cells that carry deletions in any or all of this organism's minus end–directed, microtubule-dependent motors: two related kinesin 14s (Pkl1p and Klp2p) and dynein. None of these deletions abolished biorientation, but fewer chromosomes segregated normally without Pkl1p, and to a lesser degree without dynein, than in wild-type cells. In the absence of Pkl1p, which normally localizes to the spindle and its poles, the checkpoint that monitors chromosome biorientation was defective, leading to frequent precocious anaphase. Ultrastructural analysis of mutant mitotic spindles suggests that Pkl1p contributes to error-free biorientation by promoting normal spindle pole organization, whereas dynein helps to anchor a focused bundle of spindle microtubules at the pole.

INTRODUCTION

Chromosome biorientation takes place during prometaphase, often when the chromosomes are near one of the spindle poles (reviewed in Rieder and Salmon, 1998; McIntosh *et al*., 2002; Maiato *et al.,* 2004; Tanaka *et al.,* 2005b). Subsequent movement away from that pole, i.e., congression to the metaphase plate, is effected by several spindle forces that push chromosome to the spindle midzone. Such forces can be generated by chromokinesins, which bind to chromosome arms, and by kinetochore-localized motors (Schaar *et al.,* 1997; Goshima and Vale, 2003; Mazumdar and Misteli, 2005; Zhu *et al.,* 2005). For example, the plus end–directed, kinetochore motor CENP-E contributes to the congression of a mono-oriented, pole-proximal chromosome by sliding its unattached kinetochore toward the plus ends of the nearby microtubules (MTs; Kapoor *et al.,* 2006). Such movements bring this kinetochore closer to the previously distant pole, presumably increasing its chances of binding MTs that grow from that pole. Alternatively, congression can be brought about by attachment of one of the pole-proximal sister kinetochores to MTs that grow from the distant pole (Nicklas, 1997). In this case congression is presumably driven by minus end–directed motors pulling the distal kinetochore toward the pole it faces (Savoian *et al.,* 2000; Sharp *et al.,* 2000, Schmidt *et al.,* 2005).

The fission yeast, *Schizosaccharomyces pombe*, is a powerful system for the study of mitotic processes because of its excellent genetics and cytology and because the chromosome motions in this cell resemble those of higher eukaryotes. Its fully sequenced genome includes genes for three minus end–directed, MT-dependent motors that could contribute to chromosome congression: two members of the kinesin 14 family (Pkl1p and Klp2p, Pidoux *et al.,* 1996; Troxell *et al.,* 2001) and dynein (Yamamoto *et al.,* 1999). The motor domains of Pkl1p and Klp2p are similar in sequence, both to each other and to the *Saccharomyces cerevisiae* motor Kar3p (Meluh and Rose, 1990). Klp2p resides in the cytoplasm during interphase, where it contributes to MTs sliding and cell polarity (Carazo-Salas *et al.,* 2005). Early in mitosis it moves to the kinetochores (Troxell *et al.,* 2001), where it aids the chromosome poleward motion in prometaphase by promoting processive kinetochore MT shortening (Grishchuk and McIntosh, 2006). The Kar3p motor of budding yeast has also been shown to contribute to mitotic kinetochore-MT attachments and movements (Tanaka *et al.,* 2005a; Tytell and Sorger, 2006).

The second *S. pombe* kinesin 14, Pkl1p, is localized to the nucleus throughout the cell cycle; in mitosis it is found on the spindle and spindle pole bodies (SPBs; Pidoux *et al.,* 1996). Although its importance for normal cell division has been established, the exact role of this motor is still unknown. Pkl1p enrichment at the poles and its genetic interactions with γ-tubulin suggest that it may play some role in SPB functioning (Paluh *et al.,* 2000). The third *S. pombe* minus end–directed motor, dynein (Dhc1p), drives nuclear oscillations during fission yeast meiosis (Yamamoto *et al.,* 1999). A

This article was published online ahead of print in *MBC in Press* (http://www.molbiolcell.org/cgi/doi/10.1091/mbc.E06–11–0987) on April 4, 2007.

[D] [V] The online version of this article contains supplemental material at *MBC Online* (http://www.molbiolcell.org).

Address correspondence to: Ekaterina L. Grishchuk (Katya@colorado.edu).

Abbreviations used: DAPI, 4′,6′-diamidino-2-phenylindole dihydrochloride; EM, electron microscopy; ET, electron tomography; GFP, green fluorescent protein; MT, microtubule; SPB; spindle pole body.

direct study of chromosome poleward motion during mitotic prometaphase has revealed little or no abnormality when either Dhc1p or Pkl1p was absent (Grishchuk and McIntosh, 2006). Late in mitotic division dynein and Pkl1p may be involved in localizing the checkpoint protein Mad2p to the spindle midzone (Mayer *et al.*, 2006).

At the beginning of mitosis, the kinetochores of three fission yeast chromosomes are located immediately adjacent to the duplicated SPBs (Funabiki *et al.*, 1993). This close juxtaposition may aid in the normal establishment of MT links between kinetochores and poles before SPB separation. Indeed, as soon as the spindle begins elongation, the kinetochores are already stretched between the separating poles. Such early kinetochore-SPB interactions might explain why *S. pombe* is viable and therefore often succeeds in chromosome biorientation, even in the absence of all three minus end–directed motors (Troxell *et al.*, 2001).

To explore the possible contributions of minus end–directed motors to chromosome congression and biorientation, we have studied these processes in prometaphase cells in which both sister kinetochores of chromosome 2 have become associated with one of the two, already separated spindle poles. This situation was achieved by using strains that carried the cold-sensitive allele of β-tubulin, *nda3-KM311*. Restrictive temperatures disrupt the MTs of these cells, providing a reversible arrest in early mitosis (Hiraoka *et al.*, 1984; Kanbe *et al.*, 1990). During such a block, the kinetochores of *S. pombe* frequently lose their attachment to the SPBs and diffuse away. When these cells are warmed to permissive temperatures, MTs form and move the kinetochores back to the poles (Supplementary Figure 1). During the retrieval, the kinetochores attach via MTs only to the pole to which they move (Grishchuk and McIntosh, 2006), so their subsequent biorientation requires the establishment of de novo MT links with the opposite pole. Here, we use a combination of electron tomography and fluorescent imaging of live and fixed cells to examine the congression and biorientation of the retrieved, pole-proximal kinetochores. Our results show that although the minus end–directed motors in *S. pombe* are not essential for these processes, Pkl1p and dynein contribute independently to their efficacy. We conclude that these motors are required not for chromosome motion during congression but for the normal organization and/or function of the spindle poles and their associated MTs.

MATERIALS AND METHODS

Cell Cycle Synchronization and Immunofluorescence Microscopy

S. pombe cells were grown using standard techniques and reagents (Moreno *et al.*, 1991). Cells carrying the *nda3-KM311* mutation and various motor deletions (Table 1) were synchronized in mitosis by 7–8-h incubation at 18°C. DNA was visualized with DAPI. The kinetochore marker Mis12 was visualized with anti-hemagglutinin (HA) antibodies in the strain *nda3-KM311 mis12-HA LEU2 leu1 ura4-D18 h*$^-$. Missegregation of chromosome 2 was analyzed for different motor deletions in the genetic background *nda3-KM311 mis12-HA LEU2 cen2-GFP leu1 ura4 h*$^-$. Anti-green fluorescent protein (GFP) antibodies for *cen2-GFP* immunofluorescence were kindly provided by P. Silver and J. Kahana (Harvard University, Cambridge, MA). Mad2-GFP signal was scored in cells fixed in 4% paraformaldehyde and stained with DAPI. Spindle poles were visualized with anti-Sad1 antibody (kindly provided by I. Hagan, University of Manchester, United Kingdom); mini-chromosome loss was measured as described (Halverson *et al.*, 1997; Fedyanina *et al.*, 2006). Other reagents were as described in (Grishchuk and McIntosh, 2006). Virtually all experiments were carried out using two or more independent isolates of strains with identical genotypes.

Live Cell Imaging

The centromere of chromosome 2 was visualized using a *cen2-GFP* construct, kindly provided by A. Yamamoto (Yamamoto and Hiraoka, 2003). Spindle poles were visualized using a chimera of GFP with Pcp1p, the *S. pombe* homolog of budding yeast Spc110p (Flory *et al.*, 2002). The *nda3* cells carrying both constructs were processed as described (Grishchuk and McIntosh, 2006). Images were acquired every 15 s as stacks of 7–12 planes (0.25-μm step, 150-ms exposure for each plane). In our microscope the temperature of the 100× oil immersion objective and of the water-jacket around the high NA oil condenser increased from the initial 14°C up to 32°C within 2 min, as measured by the temperature of the immersion oil on the objective lens. The Supplementary Videos show the averaged, depixelated XY-projections manually aligned to minimize the image drift brought about by the abrupt temperature change.

Electron Microscopy

Strains were grown at 18°C, as described above, then shifted to 32°C for 2–15 min, quickly collected by filtration, high-pressure frozen, and processed as previously described (Ding *et al.*, 1997; Grishchuk and McIntosh, 2006). Tomograms were computed for each of two orthogonal tilt axes and then aligned and combined (Mastronarde, 1997). Spindle MTs and SPBs were modeled using the IMOD program (Kremer *et al.*, 1996). Structural features of SPBs and MT ends were analyzed by extracting a slice of image data 1-voxel thick, using the Slicer feature of IMOD to adjust the position and orientation of the plane to obtain different views (O'Toole *et al.*, 1999).

RESULTS

Congression and Biorientation of the Pole-proximal Kinetochores Are Not Abolished in the Absence of Any or All of the Minus End–directed Motors

To examine spindle formation after the reversible disruption of MTs in strains deleted for one or more of the minus end–directed motors, cells were incubated at 18°C, the restrictive temperature for MT polymerization in the *nda3-KM311* background, and then returned to 32°C. First, we followed the separation of the SPBs, because both Pkl1p and Klp2p have been suggested to participate in establishing and maintaining normal spindle length (Pidoux *et al.*, 1996; Troxell *et al.*, 2001). In our test system, however, SPB separation in the absence of these motors was almost undelayed and occurred at the normal rate, as determined by 4D fluorescence microscopy of live cells (Figure 1A). A similar conclusion was drawn by examining the kinetics of SPB separation using fluorescence imaging of kinetochores and poles in cells fixed at different times after the temperature shift (Figure 1B).

We then used live imaging to identify cells in which the tagged chromosome moved to one of the separated spindle poles. By following such pole-proximal kinetochores, we found that they were able to congress to the spindle midplane in a majority of cells with each genotype, although the efficiency of biorientation was markedly decreased in *pkl1*Δ and *dhc1*Δ cells (Figure 1C). Interestingly, however, among the kinetochores that congressed successfully, there were no statistically significant differences in the times required for either biorientation or metaphase (Figure 1A). Thus, the absence of Pkl1p or dynein motors led to two distinct populations of cells: one in which the kinetochores failed in these processes, and another in which kinetochores congressed and bioriented in a manner that appeared perfectly normal. For example, after their initial poleward movement, the labeled kinetochores in some *pkl1*Δ cells gradually rotated around the pole and moved toward a midspindle position, just as in virtually all control and *klp2*Δ cells (Supplementary Videos 1 and 2).

Kinetochore movement to the midspindle position was also not abolished in cells that lacked all three motors (Klp2p, Pkl1p and dynein; Supplementary Video 3), showing that minus end–directed motor activity is not essential for chromosome congression in *S. pombe*. Thus, some result of Pkl1p or dynein motor deletion makes normal congression and biorientation less likely, but the minus end–directed motors are not required for these processes.

Table 1. *S. pombe* strains used in this study

Strain no.	Genotype
Strains used for immunofluorescence	
K22	*nda3* (aka *nda3-KM311*) *mis12-HA,LEU2 leu1 ura4-D18 h*$^-$
K57	*pkl1*Δ (aka *pkl1D25::his3*$^+$) *nda3 mis12-HA,LEU2 ade6 his3-D1 leu1 ura4-D18 h*$^-$
K43	*klp2*Δ (aka *klp2*Δ*::ura4*$^+$) *nda3 mis12-HA,LEU2 ade6-M210 his3-D1 leu1 ura4-D18 h*$^-$
McI#615	*dhc1*Δ (aka *dhc1-d4::ura4*$^+$) *nda3 mis12-HA,LEU2 leu1 ura4-D18 h*$^-$
K62	*nda3 mis12-HA,LEU2 cen2-GFP* (aka *cen2::kan*^{r}*-ura4*$^+$*-lacOp his7*$^+$*::lacI-GFP*) *leu1 ura4-D18 h*$^-$
K94	*pkl1*Δ *nda3 mis12-HA,LEU2 cen2-GFP leu1 ura4-D18 h*$^-$
K90	*klp2*Δ *nda3 mis12-HA,LEU2 cen2-GFP leu1 ura4-D18 h*$^-$
K91	*dhc1*Δ *nda3 mis12-HA,LEU2 cen2-GFP leu1 ura4-D18 h*$^-$
K95	*pkl1*Δ *klp2*Δ *nda3 mis12-HA,LEU2 cen2-GFP leu1 ura4-D18 h*$^-$
K93	*pkl1*Δ *dhc1*Δ *nda3 mis12-HA,LEU2 cen2-GFP leu1 ura4-D18 h*$^-$
K48	*nda3 mis12-HA mad2-GFP::kan*^{R} *leu1-32 ura4-D18 h*$^-$
McI#699	*pkl1*Δ *nda3 mis12-HA mad2-GFP::kan*^{R} *leu1-32 ura4-D18 h*$^-$
Strains used for live imaging	
K64	*nda3 cen2-GFP pcp1-GFP* (aka *nmt1-GFP-pcp1*$^+$*::kan*^{r}) *leu1-32 ura4 h*$^-$
K69	*pkl1*Δ *nda3 cen2-GFP pcp1-GFP leu1-32 ura4 h*$^-$
K70	*klp2*Δ *nda3 cen2-GFP pcp1-GFP leu1-32 ura4 h*$^-$
K71	*dhc1*Δ *nda3 cen2-GFP pcp1-GFP leu1-32 ura4 h*$^-$
K106	*pkl1*Δ *dhc1*Δ *nda3 cen2-GFP pcp1-GFP leu1-32 ura4 h*$^-$
K118	*pkl1*Δ*klp2*Δ *dhc1*Δ *nda3 cen2-GFP pcp1-GFP leu1-32 ura4 h*$^-$
Strains used for a mini-chromosome loss assay	
McI#409	*ade6-704 leu1-32 ura4-D18 h*$^+$*/minichr* (aka *pSp(cen1–7L)sup3E ura4*$^+$)
McI#706	*pkl1*Δ *ade6-704 leu1-32 ura4-D18 h*$^-$*/minichr*
McI#702	*klp2*Δ *ade6-704 leu1-32 ura4-D18 h*$^-$*/minichr*
McI#704	*dhc1*Δ *ade6-704 leu1-32 ura4-D18 h*$^-$*/minichr*
McI#711	*pkl1*Δ *klp2*Δ *ade6-704 leu1-32 ura4-D18 h*$^-$*/minichr*
McI#714	*pkl1*Δ *dhc1*Δ *ade6-704 leu1-32 ura4-D18 h*$^-$*/minichr*
McI#712	*klp2*Δ *dhc1*Δ *ade6-704 leu1-32 ura4-D18 h*$^+$*/minichr*
McI#707	*pkl1*Δ *klp2*Δ *dhc1*Δ *ade6-704 leu1-32 ura4-D18 h*$^+$*/minichr*
Other strains	
K114	*dhc1*Δ *cut7-21 leu1-32 ura4-D18 h?*
K115	*dhc1*Δ *cut7-24 ade6 leu1-32 ura4-D18 h?*
McI#693	*pkl1*Δ *mad2*Δ*::ura4*$^+$ *leu1-32 ura4-D18 h*$^-$
McI#694	*pkl1*Δ *bub1*Δ*::ura4*$^+$ *ade6-M216 leu1-32 ura4 h*$^-$

Certain original strains with tagged constructs were kindly provided by A. Yamamoto and Y. Hiraoka (Kansai Advanced Research Center, Japan) (*cen2-GFP* and *dhc1D-d4*), G. Goshima and M. Yanagida (Kyoto University, Japan) (*mis12-HA*), M. Flory and T. Davis (University of Washington, Seattle, WA) (*pcp1-GFP*), T. Troxell and J. R. McIntosh (University of Colorado, Boulder) (*pkl1*Δ and *klp2*Δ), T. Toda (London Research Institute, United Kingdom) (*mad2GFP*), L. Clarke (University of California, Santa Barbara, CA) (strain with mini-chromosome), I. Hagan (*cut7*^{ts}), and S. Sazer (Baylor College of Medicine, Houston, TX) (*mad2*Δ).

When Chromosomes Fail to Congress and Biorient in the Absence of Pkl1p, Anaphase Initiation Is Not Delayed

Previous analysis of the mitotic progression in *pkl1*Δ *nda3* cells revealed a slight advancement in the average time of anaphase initiation (Grishchuk and McIntosh, 2006). To examine the consequences of such precocious mitotic exit we measured the viability of this and other motor deletion strains during the synchronization procedure. The strains lacking *pkl1*$^+$ had noticeably lower viability than all other strains examined, even when grown at 32°C (permissive conditions for the mutant tubulin; Figure 1D). There was a further decrease in cell survival after incubation at restrictive temperature relative to survival before the arrest (48%). The precocious anaphase initiation, combined with the decreased viability of *pkl1*Δ cells, suggested that the deletion of Pkl1p abrogated a mitotic checkpoint. This effect was unlikely to have resulted from problems with spindle formation, because as described above, the rates of SPB separation were statistically indistinguishable in all these strains.

In all strains we have examined, there were occasionally kinetochores that failed to biorient within the duration of the experiment (up to 40 min). In control cells, or those lacking Klp2p or dynein, the inability of a chromosome to leave the pole with which it first associated was accompanied by a delay in anaphase onset (Supplementary Video 4). However, in *pkl1*Δ cells spindle elongation was frequently not delayed: in 4 of 5 cells with pole-proximal kinetochores anaphase spindle elongation began 10.5 ± 2.4 min after kinetochore retrieval, even though the tagged kinetochore failed to congress and biorient (Supplementary Video 5). This time is identical to the duration of metaphase in control cells (10.1 ± 2.1 min). Because sample size from live cell imaging is limited, we analyzed the missegregation frequency of chromosome 2 in fixed cell cultures by scoring the percent of late anaphase cells in which both *cen2* signals were in one daughter nucleus (Figure 1E). In *pkl1*Δ cells chromosome 2 missegregated more frequently than in control cells or in those with deletions of the *klp2* or *dhc1* genes (Figure 1F). Apparently, the premature mitotic exit seen in fixed cultures of *pkl1*Δ cells, the decreased cell viability, and the elevated chromosome missegregation all resulted from the inability of pole-proximal kinetochores to block anaphase spindle elongation in the absence of Pkl1p motor.

Pkl1p Does Not Play a Direct Role in the Mad2-dependent Checkpoint Pathway

One possibility for how a deletion in a minus end–directed motor could lead to abnormal mitotic checkpoint control is

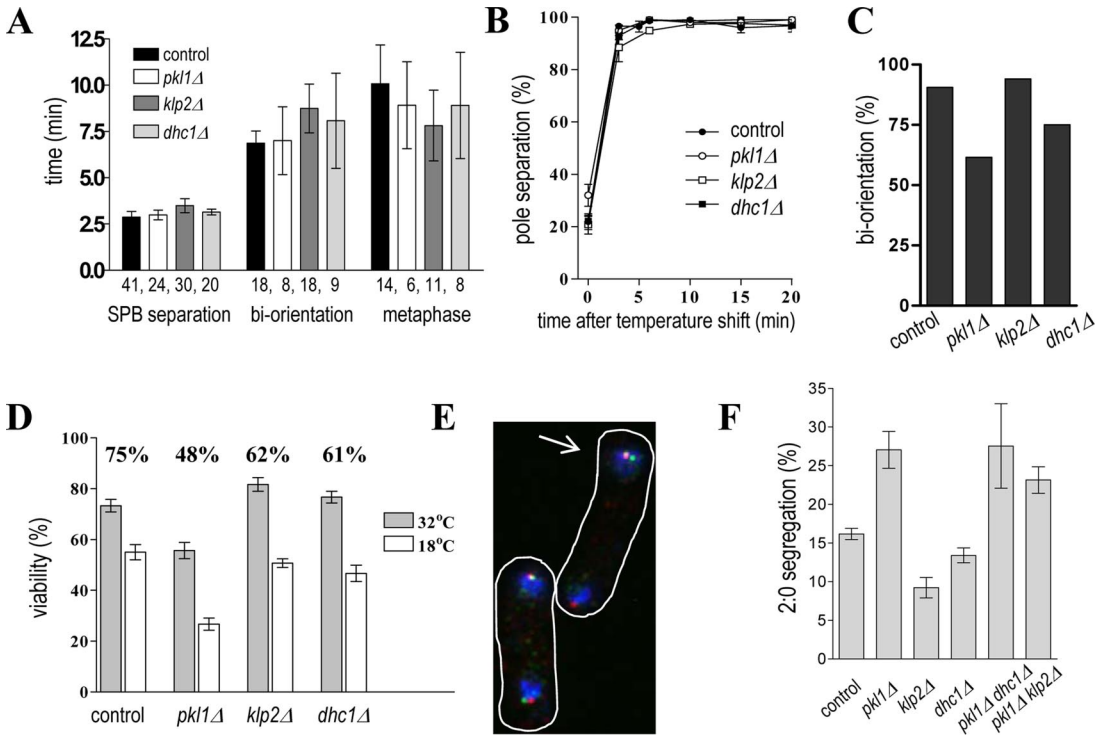

Figure 1. Mitotic progression and chromosome segregation in motor mutants. (A) Average duration of different mitotic processes, as seen via live cell, 4D imaging. Error bars on all figures are SEMs with 95% confidence. Number of measurements in each category is given below the corresponding bars. Zero time for each measurement was when we initiated specimen warming. SPB separation was defined as the first time when the two poles could be resolved as separate objects. Bi-orientation was the time interval between a kinetochore's arrival at a pole and the first time it was seen at the midpoint between the separated poles. The attachment of sister kinetochores to sister poles was evident from kinetochores stretching and their subsequent movement to opposite poles in anaphase. Metaphase lasted from kinetochore biorientation until anaphase onset. Kinetochores that failed to congress or to start anaphase during the recording time (25–40 min) were not included. (B) Kinetics of SPB separation as determined in fixed cultures. The ordinate shows the percent of cells with condensed, unseparated chromosomes in which two SPBs could be detected. Poles were visualized with antibodies to the SPB marker Sad1. The data are from three or more independent experiments in each of which >100 cells of each genotype were counted. (C) Efficiency of kinetochore biorientation. Percent of cells in which kinetochores congressed to spindle midzone during the recording time. Number of cells viewed: control, 21; *pkl1*Δ, 12; *klp2*Δ, 17; and *dhc1*Δ,12. (D) Cell viability was determined in at least three independent experiments by plating a fixed number of cells before (▨) and after the arrest (□). After growth at 32°C, the number of colonies was counted, and viability was expressed as a percent of the expected number of colonies, based on the number of cells plated. Numbers above the bars are the percent of cells surviving after the cold block, expressed relative to those surviving before the block. (E) The sister kinetochores of chromosome 2 (green) were sometimes found in only one of two late anaphase nuclei (2:0 segregation, arrow). DNA is stained with DAPI (blue), and all three kinetochores are stained in red using an antibody to the kinetochore-specific protein Mis12-HAp. *Cen2-GFP* marker was visualized using an anti-GFP. Cells boundaries are drawn for clarity. (F) The percent of late anaphase cells with 2:0 segregation of *cen2* in different genetic backgrounds. In control cultures the percent of such cells was higher than expected from the reported frequency of chromosome loss in wild-type cells (Bodi *et al.*, 1991). This is likely to result both from the synchronization procedure and from the difficulty of distinguishing the event of interest from missegregations due to the extensive scatter of chromosomes during the arrest (Grishchuk and McIntosh, 2006).

that this motor is involved in the transport or regulation of an important checkpoint component. At least two kinetochore-localized motors, CENP-E and dynein, are known to contribute directly to checkpoint inactivation, in the latter case by removing Mad2 from the bioriented kinetochores (Mao *et al.*, 2005; Howell *et al.*, 2001). If Pkl1p too were involved in checkpoint inactivation, cells deleted for this gene would be expected to arrest in mitosis and delay anaphase initiation, a phenotype that is opposite to the one observed. To further examine the checkpoint deficiency in *pkl1*Δ cells, we determined the localization of Mad2 protein in these cells synchronized via the *nda3-KM311* mutation. When these cells were subjected to our customary low-temperature mitotic arrest, which depolymerizes essentially all of the cell's MTs (Grishchuk and McIntosh, 2006), their condensed chromosomes often contained 2–3 bright fluorescent spots of Mad2-GFP, indicating a normal recruitment of this checkpoint component to the unattached kinetochores (Figure 2A; Ikui *et al.*, 2002). After a shift to the permissive temperature, the *pkl1*Δ *nda3-KM311 mad2-GFP* cells exited mitosis slightly faster than control cells, and the percentage of cells with Mad2-GFP bright dots also decreased fast (Figure 2, B and C). Thus, Pkl1p plays no detectable role in deactivating the checkpoint via the reduction of Mad2 levels during prometaphase.

In anaphase, Mad2-GFP was seen as weak dots at one or both ends of the spindle (Ikui *et al.*, 2002; Garcia *et al.*, 2002; Saitoh *et al.*, 2005), and unlike a previous report (Mayer *et al.*, 2006), this pattern was unaffected by the absence of Pkl1p (Figure 2D). Furthermore, only 1 of 17 anaphase cells with unequal daughter nuclei (such as in Figure 1E) exhibited a relatively bright Mad2-GFP signal in the larger nucleus. Thus, despite apparently faulty chromosome attachments, the kinetochores of the missegregating, pole-proximal chromosome have normal, reduced levels of Mad2, which is likely to explain their failure to inhibit anaphase initiation.

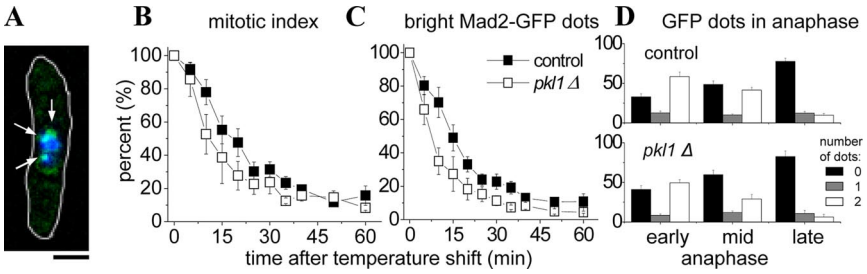

Figure 2. Localization of the checkpoint protein Mad2-GFP. (A) During mitotic arrest, the bright fluorescent speckles of Mad2-GFP (green) are seen in 91 and 85% of the control and *pkl1*Δ cells, respectively, that have condensed, unseparated chromosomes (stained with DAPI, blue). Bar, 2 μm. Cell boundaries are shown for clarity. After shift to permissive temperature, cells exit mitosis, as seen from the decrease in percent of cells with condensed, unseparated chromosomes (B) and with bright green speckles (C). The data were collected from four independent experiments in which 200 cells were counted for each time. Numbers are expressed as percent from values at time 0. (D) The fluorescent dots (presumably colocalizing with SPBs and/or their associated kinetochores) were scored in early anaphase cells, in which DNA masses were separated by 1.5–3 μm (sizes characteristic of daughter DNA masses), and in late anaphase when two nuclei were at the distal cell ends. All other anaphase configurations were scored as midanaphase. Signal brightness decreased fast, and by the end of anaphase virtually all cells had no Mad2-GFP chromosome-associated dots. The differences between control and *pkl1*Δ anaphase cells were not significant.

Consistent with the lack of evidence for the checkpoint activation in these cells, growth of the *pkl1*Δ cells was unaffected by the deletion of either *mad2* or *bub1* genes.

The Increase in Chromosome Loss in pkl1Δ Correlates with a Disorganized SPB

To seek other explanations for the anaphase initiation in *pkl1*Δ cells with pole-proximal chromosomes, we have used electron tomography (ET) to examine structural features of the mitotic spindles formed in the absence of Pkl1p. Cells with deletions in the minus end–directed motor enzymes were synchronized using the *nda3-KM311* mutation and were high-pressure frozen several minutes after their release from the cold temperature block (see *Materials and Methods*). The reconstructed spindles in *pkl1*Δ and *dhc1*Δ cells looked fairly normal (based on 3 and 5 full reconstructions, respectively), but the morphology of spindle poles in *pkl1*Δ cells was distinctly abnormal. Fission yeast SPBs are normally prominent, plaque-like structures that enter a fenestra in the nuclear envelope during mitosis (Ding *et al.*, 1997). They are associated with a diffuse "bridge" on the cytoplasmic side of the nuclear envelope (Figure 3, A and B; Uzawa *et al.*, 2004). Figure, 3, C and C′, shows slices from a tomogram of a *pkl1*Δ *nda3* pole whose overall structure looks normal. However, the second pole in this cell did not have a plaque, although both poles had a normal-looking "bridge" (Figure 3, D and D′).

In another *pkl1*Δ *nda3* cell with an early prometaphase spindle, one of the poles appeared normal, but the other again lacked the normal, plaque-like structure (Figure 4, A and B). The area near this pole was occupied by a well-

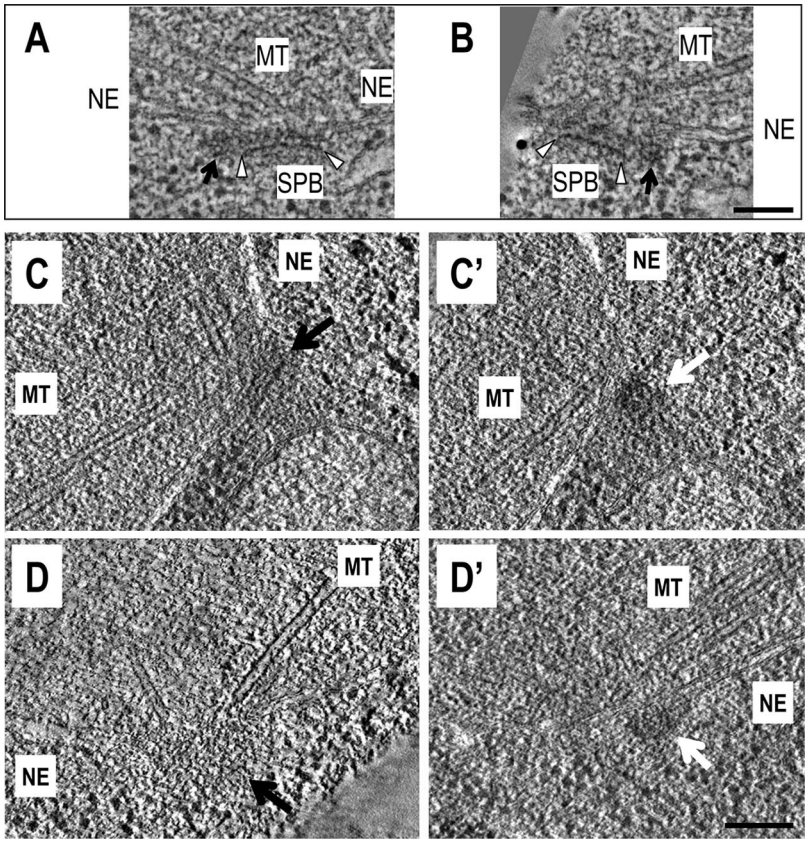

Figure 3. Ultrastructural analysis of SPB morphology. (A and B) Slices from tomographic reconstruction of two SPBs from an *nda3* cell frozen several minutes after the shift to 32°C. The SPBs sit slightly outside an opening (fenestra) in the nuclear envelope (NE). They are layered structures that include a dark-staining plaque (the curved line marked by white arrowheads), surrounded by a loosely structured felt-work of fibrous material. MTs are on the nucleoplasmic side of the plaque. Arrows point to "half-bridges," which lie at the edges of the SPBs. (C and D) Tomographic slices from a *pkl1*Δ *nda3* spindle, showing both spindle poles. The nuclear envelope in this cell looks normal, but one of the SPBs (D) lacks the normal plaque morphology that is visible at the other pole on C (black arrows). Note that the 3D images from ET have allowed us to look at these poles from all orientations and at every level contained in 2–3 adjacent 250-nm tomographic slices, so the absence of an observable plaque is significant. Both poles do have apparently normal bridge structures outside NE (C′ and D′, white arrows). Bar, 100 nm.

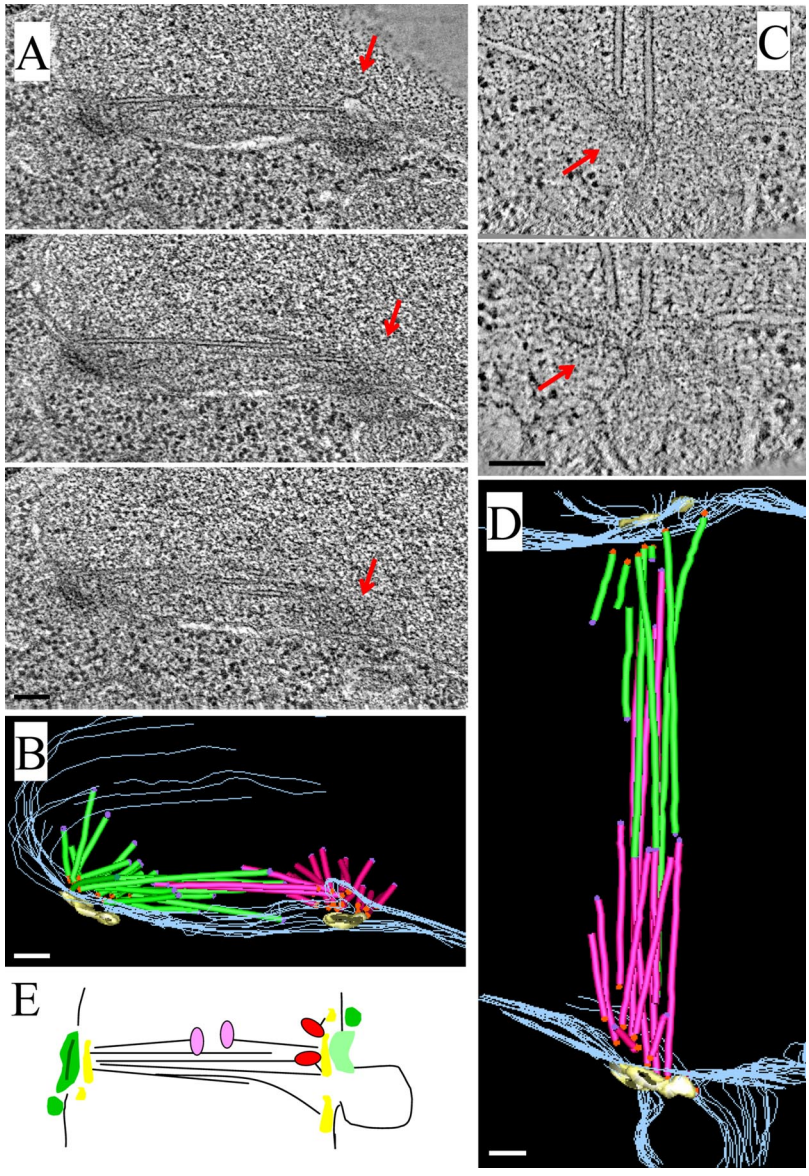

Figure 4. Abnormal pole structure in the absence of Pkl1p. Neighboring tomographic slices (A and C) and 3D models (B and D) from tomograms of two *pkl1*Δ *nda3* spindles (see Supplementary Videos 6 and 7, respectively). Red arrows point to poles with abnormal morphology. Bar, 100 nm. (E) Summary diagram of suggested abnormal kinetochore-pole attachment in *pkl1*Δ cells. Normally, sister kinetochores (pink) attach to sister SPBs (green). If, however, a pole fragments, the MT-nucleating material (yellow) might form an ectopic area, so two sister kinetochores (red) could attach to different areas of the same pole. Such an abnormal biorientation would be expected to have a normal number of kinetochore MTs (although their shortness would be an obstacle in their detection), and the structure might either saturate enough kinetochore MT-binding sites or generate sufficient tension to silence the checkpoint.

stained, structure-less material, and spindle MTs originated from beside this area at a small, abnormal evagination of the nuclear envelope (Supplementary Video 6). A similar configuration was found in a cell of the same genotype that contained a longer spindle (Figure 4, C and D); here the evagination was much larger (Supplementary Video 7). Again, MTs emanated from the diffuse, envelope-associated area that lacked normal pole morphology; the resulting spindle MTs appeared less focused and bundled than normal.

The majority of the MT minus ends in this and other cells examined looked normal, and the number of the MTs growing from the two poles was very similar (Supplementary Figure 2). Thus, in spite of its genetic interaction with γ-tubulin (Paluh *et al.*, 2000), Pkl1p is unlikely to be involved directly in either MT nucleation or in the anchoring of MT ends at the pole. Instead, this motor appears to contribute to the maintenance of overall pole structure. If a pole becomes prone to partial fragmentation in the absence of Pkl1p, the resulting ectopic areas of MT nucleation could promote abnormal biorientation to that pole alone. It is likely that such an attachment could escape the checkpoint machinery (Figure 4E; see *Discussion*).

Absence of Dynein Leads to Rare Defects in Biorientation and Chromosome Segregation, as well as to a Less Efficient MT Bundling at the SPB

Although intracellular protein levels of dynein heavy chain are low and the localization of this protein in mitosis is still unknown, the expression of the *dhc1*$^+$ gene is readily detectable in vegetative cells (Supplementary Figure 3). Using the above assays, we established that *dhc1*Δ cells had normal kinetics of mitotic progression (Figure 1, A and B) and normal levels of both viability and chromosome 2 missegregation (Figure 1, D–F). However, examination of biorientation in live *dhc1*Δ *nda3* cells revealed some subtle but detectable abnormalities (Figure 1C). For example, the pole-proximal kinetochore in *dhc1*Δ cells frequently moved away from the pole, often not toward the opposite pole, so up to three fluorescent spots could be resolved simultaneously (Supplementary Video 8). In contrast, in cells of other geno-

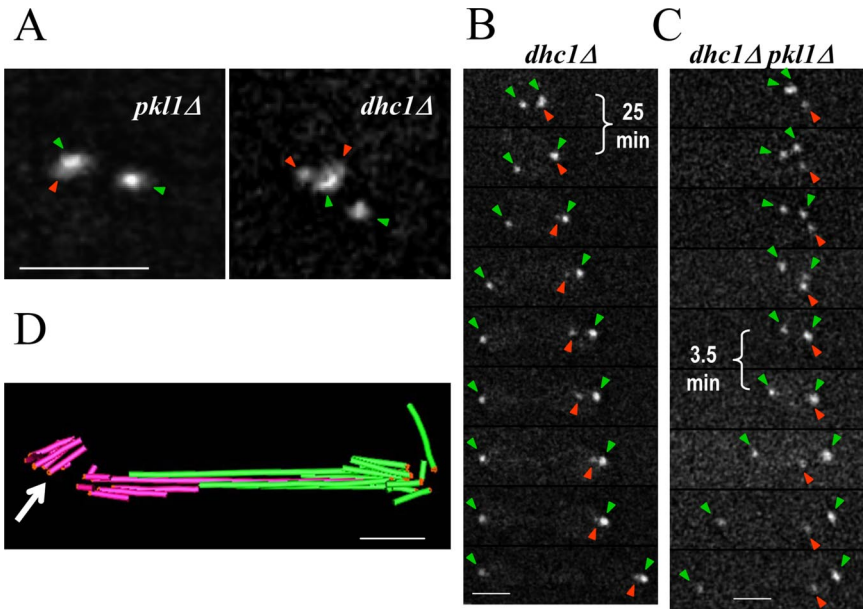

Figure 5. Chromosome biorientation is impeded by the absence of dynein. (A) Sample frames showing the positions of a pole-proximal kinetochore in a *pkl1*Δ (Supplementary Video 5) and a *dhc1*Δ (Supplementary Video 8) cell. In *pkl1*Δ the kinetochore lies immediately beside one pole (green arrowhead), whereas in *dhc1*Δ two sister kinetochores (red arrowheads) can be seen near the brighter SPB signal. Bar, 2 μm. (B and C) Selected live images showing anaphase spindle elongation in *dhc1*Δ *nda3* and *dhc1*Δ *pkl1*Δ *nda3* cells, respectively. In B, two sister kinetochores of chromosome two (red arrowhead) are at the pole on the right, which is consequently brighter. The dim signal appearing between the poles in anaphase is likely to represent a single sister kinetochore of the missegregating chromosome 2. Both spindles on B and C elongate in the absence of normal biorientation, but the important difference is that in the *dhc1*Δ cell anaphase starts after a 25-min delay, whereas in the *dhc1*Δ *pkl1*Δ double mutant anaphase starts 3.5 min after the kinetochore's retrieval. (D) 3D model of the *dhc1*Δ *nda3* spindle with a split kinetochore bundle (arrow). See also Supplementary Video 10.

types, in which the kinetochore was at the pole for an extended time, the *cen2-GFP* signal remained closely associated with the pole (Figure 5A; Supplementary Video 4). In two *dhc1*Δ cells that failed in congression, anaphase eventually started (>34 min after kinetochore retrieval in Supplementary Video 9), but unlike in *pkl1*Δ cells, one of the sister kinetochores lagged transiently behind the moving pole (Figure 5B).

EM tomography of *dhc1*Δ cells showed normal overall morphology of the spindle and SPBs. Only 1 of 5 fully reconstructed spindles had a distinctly abnormal feature (Figure 5D), which we have not encountered in 12 additional, full-spindle reconstructions from cells of other genotypes. The pole-associated MTs on one side of the spindle were separated into two bundles (arrow). Moreover, the minus ends of the MTs in the interdigitating core bundle were farther from the SPB, and the second bundle was turned sideways (Supplementary Video 10). Such splitting of the MT bundles could have made a looser, less cohesive kinetochore-SPB association, accounting for the abnormal motions of the pole-proximal kinetochores seen in live *dhc1*Δ cells.

Dynein and Pkl1p Contribute to Chromosome Biorientation via Different Pathways

Deletion of the $pkl1^+$ gene is known to suppress the temperature sensitivity of growth in $cut7^{ts}$ cells (kinesin 5) in allele-specific manner (Pidoux *et al.*, 1996, Troxell *et al.*, 2001). To examine whether Pkl1p and dynein promote chromosome biorientation via the same pathway, we have carried out the analysis of tetrads from genetic crosses between *dhc1*Δ and the temperature-sensitive strains *cut7–21* and *cut7–24*; these two alleles are suppressed in the strongest and weakest manner, respectively, by the $pkl1^+$ and $klp2^+$ deletions (Troxell *et al.*, 2001). Temperature sensitivity (25–36°C range) of both, *cut7–21* and *cut7–24* strains, was unchanged in the *dhc1*Δ background, suggesting that dynein and Pkl1p work in different mitotic pathways.

Because chromosome congression and biorientation were partially impeded by the absence of either dynein or Pkl1p, we then asked if there was an enhanced defect in their double deletion. The rate of *cen2* missegregation in this strain was identical to that seen in *pkl1*Δ alone (Figure 1F). Live imaging of the double mutant cells revealed characteristics of each single mutant: premature anaphase in the absence of biorientation (*pkl1*Δ phenotype), and a loose kinetochore-pole association as seen by kinetochore lagging in anaphase (*dhc1*Δ phenotype; Figure 5C). Similar additive behavior was also seen in *dhc1*Δ *pkl1*Δ *klp2*Δ cells. For example, after the kinetochore was retrieved in this triple deletion strain (Supplementary Video 11), the spindle began elongation even though this kinetochore had failed to congress and biorient. These results suggest that dynein and Pkl1p contribute to chromosome biorientation by distinct and perhaps nonredundant mechanisms.

The above observations were carried out in the presence of a conditional allele of β-tubulin, so we also examined roles of the minus end–directed motors in chromosome segregation by measuring the rate of a mini-chromosome loss in *S. pombe* cells carrying the wild-type *nda3* gene (strains listed in Table 1). Consistent with the above conclusions, mini-chromosome loss was unaffected by the $klp2^+$ deletion, and it was increased fourfold in the absence of dynein: $1.2 \pm 0.2 \times 10^{-3}$ losses per division in *dhc1*Δ cells versus $3.1 \pm 1 \times 10^{-4}$ in control cells (Figure 6). Deletion of Pkl1p led to the highest rate of the mini-chromosome loss among all single motor deletions: this strain showed a ~25-fold increase relative to wild-type cells. Thus, the minus end–directed motors Pkl1p, and to a lesser degree dynein, contribute to the accuracy of chromosome segregation independently of the *nda3-KM311* mutation. Furthermore, because the mini-chromosome was lost only slightly more frequently in *pkl1*Δ *dhc1*Δ cells than in *pkl1*Δ cells, these two motors are likely to contribute independently to the accuracy of chromosome segregation. Surprisingly, there was a twofold increase in the mini-chromosome loss in *pkl1*Δ *klp2*Δ cells relative to the *pkl1*Δ cells alone (Figure 6), although our direct measurement of *cen2* missegregation has revealed no interaction between these mutations (Figure 1F). It appears that Pkl1p and Klp2p might share some important mitotic function, other than in kinetochore congression and biorientation.

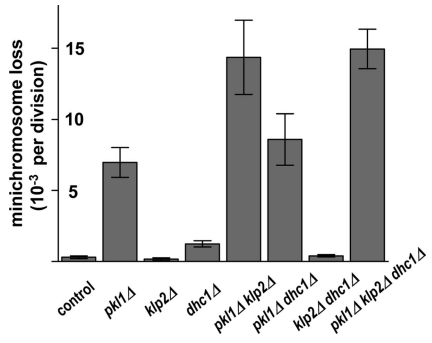

Figure 6. Frequency of the mini-chromosome loss. All strains (listed in Table 1) had a wild-type copy of the *nda3* gene and carried the mini-chromosome *pSp(cen1)-7L-sup3E* (Halverson *et al.,* 1997). More than 13,500 colonies were examined for each strain for a total of at least four independent platings.

DISCUSSION

We have used ET, live cell imaging, and immunofluorescence to study the roles of three *S. pombe* motors in chromosome biorientation. The congression of a labeled kinetochore to the midspindle position in single deletion strains, as well as in the strain that lacked all three minus end–directed motors, appeared normal in most of the cells from each genotype. These processes were completely unperturbed in the absence of Klp2p, although this motor contributes to the processivity of poleward kinetochore movement (Grishchuk and McIntosh, 2006). Together, these results strongly suggest that congression in *S. pombe* does not rely exclusively on minus end–directed motility. This conclusion is consistent with a conspicuous absence of long spindle MTs (other than those of the interpolar spindle bundle) that end in the vicinity of the opposite pole, where pole-proximal kinetochores are seen via live imaging (based on 17 full ET reconstructions of the prometaphase spindles). Such MTs would be expected to be common if their attachment to a pole-proximal kinetochore were necessary for its congression. Thus, it appears likely that chromosome congression in *S. pombe* is largely promoted by some other forces, such as those that push the kinetochores toward the metaphase plate (e.g., by a chromokinesin or plus end–directed, kinetochore-associated kinesins). Our study has also revealed that successful chromosome biorientation in *S. pombe* depends on the normal organization and functioning of the spindle poles. In particular, two minus end–directed motors, dynein and Pkl1p, contribute independently to normal pole and spindle structure.

The distinct, albeit subtle abnormalities in spindle organization in *dhc1*Δ cell (Figure 5D; Supplementary Video 10), suggest that dynein contributes to spindle organization by promoting MT bundling and by anchoring MT minus ends. Such an interpretation is consistent with a previously described role for dynein in other cell types (Heald *et al.,* 1996; Gaglio *et al.,* 1997; Walczak *et al.,* 1998; Goshima and Vale, 2003; Goshima *et al.,* 2005; Morales-Mulia and Scholey, 2005). If dynein works in *S. pombe* to transport kinetochore fibers to the pole, the less tight association of the kinetochore fibers with a pole that would result from its absence might explain the more mobile behavior of pole-associated kinetochores (Figure 5A; Supplementary Video 8), as well as the lagging of chromosomes during anaphase (Figure 5, B and C; Supplementary Video 9), and an occasional failure in chromosome biorientation (Figures 1C and 6).

The importance of the pole's normal functions in achieving accurate kinetochore biorientation is further highlighted by the phenotype of the Pkl1p deletion. Early in mitosis the spindle poles should slide apart, while situated in fenestrae within the nuclear envelope. It is likely that during their separation, the SPBs experience forces (while interacting with each other and the kinetochores) that push and pull their different parts in various directions. In the absence of Pkl1p such activities may result in the disorganization of polar material. Likewise, the regions of nuclear envelope that become distorted in this mutant may have responded to normal mitotic forces whose action could not be contained in the absence of this kinesin-14. We propose that Pkl1p, which localizes to the spindle and its poles (Pidoux *et al.,* 1996), plays a role in maintaining the coherence of the spindle pole material, analogues to that suggested or implied for other members of this family, e.g., Ncd in *Drosophila* (Goshima *et al.,* 2005) and KifC1/HSET and CHO2 in mammalian cells (Kuriyama *et al.,* 1995; Gordon *et al.,* 2001; Chakravarty *et al.,* 2004; Zhu *et al.,* 2005). The finding that in three fully reconstructed *pkl1*Δ *nda3* spindles only one of the two poles was markedly disrupted suggests that either the mother or the daughter pole is more prone to fragmentation in this genetic background. This supposition could not be tested by EM tomography, because we were unable to find duplicated but unseparated poles in our preparations, in spite of a serious search for them.

Although an apparently normal, bipolar spindle can still form in the absence of Pkl1p and distant kinetochores are retrieved normally, the poles in these cells are not completely functional; an improperly attached kinetochore can escape detection by the checkpoint system. Previous studies of *S. pombe* have shown that kinetochores that are not attached to MTs are readily detected by the checkpoint mechanism, so long as they are in the same nucleus as the metaphase spindle (Grishchuk and McIntosh, 2006). Anaphase spindle elongation was inhibited by such unattached chromosomes in control cells, as well as in those with other motor deletions, including *pkl1*Δ. Consistently, the recruitment of the Mad2 checkpoint protein to the unattached kinetochores appeared to be normal, even in the absence of Pkl1p (Figure 2). In contrast, after the chromosome had been pulled to one of the poles in *pkl1*Δ cells, Mad2 left the kinetochores; after the normal duration for metaphase the anaphase spindle began to elongate in the absence of biorientation. Although our data do not exclude the possibility that Pkl1p is involved in activation of some other important checkpoint protein, the defects we have observed in the organization of *pkl1*Δ SPBs provide an alternative explanation for such checkpoint deficiency. Indeed, if the pole is fragmented, two sister kinetochores might become syntelically attached but stably stretched between different parts of the same pole (red ovals on Figure 4E), thus avoiding detection by the checkpoint machinery.

With an increasing number of motor deletions, the details of mitotic progression change; cells carrying deletions in all three minus end–directed motors assume phenotypic features of each of the single deletion strains. Although this leads to more variability in each mitotic feature, such as kinetochore kinematics, the duration of different mitotic phases, spindle length dynamics, and the elevated rate of mini-chromosome loss, the overall parameters of mitotic progression in populations of cells with different genotypes remained surprisingly unperturbed in the absence of the minus end–directed motors. The fine deviations from normal that are sometimes seen are hard to generalize (e.g., compare control and triple deletion cells in Supplementary

Videos 1 and 3), but cells lacking the Pkl1p motor are an exception. These cells are measurably less viable (Figure 1D) and fail in accurate chromosome segregation more frequently (Figures 1F and 6), most likely as a direct consequence of their checkpoint failure. We therefore conclude that none of the major kinetochore motions during kinetochore congression and biorientation in *S. pombe* is driven exclusively by minus end–directed motors; instead, these motors improve the quality and stability of essential spindle components, such as the centrosome. Minus end–directed motor enzymes appear not to be at the root of minus end–directed, spindle-mediated motility, but their presence improves the quality and reliability of such motions. As such, they confer a significant adaptive value to chromosome segregation, whose essence is the fidelity of the final product, not the speed or economy of action.

ACKNOWLEDGMENTS

The EM tomography was done in the Boulder Laboratory for 3D electron microscopy of cells and was supported by National Institutes of Health Grant RR000592 to J.R.M. M. Morphew prepared the samples for electron microscopy, and E. O'Toole and other members of this lab helped with data acquisition and reconstruction. The temperature control for the light microscope was built by V. Sarbash and F. Ataullakhanov. We are grateful to V. Volkov for excellent technical assistance, M. Kay for help with viability experiments, V. Sridharan and R. Singh for help with RT-PCR, and M. Winey for discussions. Strains and reagents were kindly provided by Drs. I. Hagan, P. Silver, Y. Hiraoka, M. Yanagida, A. Yamamoto, T. Toda, L. Clarke, S. Sazer and T. Davis. This work was supported in part by National Institutes of Health Grant GM33787 to J.R.M. who has been a Research Professor of the American Cancer Society.

REFERENCES

Bodi, Z., Gysler-Junker, A., and Kohli, J. (1991). A. quantitative assay to measure chromosome stability in *Schizosaccharomyces pombe.* Mol. Gen. Genet. *229*, 77–80.

Carazo-Salas, R. E., Antony, C., and Nurse, P. (2005). The kinesin Klp2 mediates polarization of interphase microtubules in fission yeast. Science *309*, 297–300.

Chakravarty, A., Howard, L., and Compton, D. A. (2004). Mechanistic model for the organization of microtubule asters by motor and non-motor proteins in a mammalian mitotic extract. Mol. Biol. Cell *15*, 2116–2132.

Ding, R., West, R. R., Morphew, D. M., Oakley, B. R., and McIntosh, J. R. (1997). The spindle pole body of *Schizosaccharomyces pombe* enters and leaves the nuclear envelope as the cell cycle proceeds. Mol. Biol. Cell *8*, 1461–1479.

Fedyanina, O. S., Mardanov, P. V., Tokareva, E. M., McIntosh, J. R., and Grishchuk, E. L. (2006). Chromosome segregation in fission yeast with mutations in the tubulin folding cofactor D. Curr. Genet. *50*, 281–294.

Flory, M. R., Morphew, M., Joseph, J. D., Means, A. R., and Davis, T. N. (2002). Pcp1p, an Spc110p-related calmodulin target at the centrosome of the fission yeast *Schizosaccharomyces pombe.* Cell Growth Differ. *13*, 47–58.

Funabiki, H., Hagan, I., Uzawa, S., and Yanagida, M. (1993). Cell cycle-dependent specific positioning and clustering of centromeres and telomeres in fission yeast. J. Cell Biol. *121*, 961–976.

Gaglio, T., Dionne, M. A., and Compton, D. A. (1997). Mitotic spindle poles are organized by structural and motor proteins in addition to centrosomes. J. Cell Biol. *138*, 1055–1066.

Garcia, M. A., Koonrugsa, N., and Toda, T. (2002). Spindle-kinetochore attachment requires the combined action of Kin I-like Klp5/6 and Alp14/Dis1-MAPs in fission yeast. EMBO J. *21*(22), 6015–6024.

Gordon, M. B., Howard, L., and Compton, D. A. (2001). Chromosome movement in mitosis requires microtubule anchorage at spindle poles. J. Cell Biol. *152*, 425–434.

Goshima, G., and Vale, R. D. (2003). The roles of microtubule-based motor proteins in mitosis: comprehensive RNAi analysis in the *Drosophila* S2 cell line. J. Cell Biol. *162*, 1003–1016.

Goshima, G., Nedelec, F., and Vale, R. D. (2005). Mechanisms for focusing mitotic spindle poles by minus end-directed motor proteins. J. Cell Biol. *171*, 229–240.

Grishchuk, E. L., and McIntosh, J. R. (2006). Microtubule depolymerization can drive poleward chromosome motion in fission yeast. EMBO J. *25*, 4888–4896.

Halverson, D., Baum, M., Stryker, J., Carbon, J., and Clarke, L. (1997). A centromere DNA-binding protein from fission yeast affects chromosome segregation and has homology to human CENP-B. J. Cell Biol. *136*, 487–500.

Heald, R., Tournebize, R., Blank, T., Sandaltzopoulos, R., Becker, P., Hyman, A., and Karsenti, E. (1996). Self-organization of microtubules into bipolar spindles around artificial chromosomes in *Xenopus* egg extracts. Nature *382*, 420–425.

Hiraoka, Y., Toda, T., and Yanagida, M. (1984). The NDA3 gene of fission yeast encodes β-tubulin: a cold-sensitive nda3 mutation reversibly blocks spindle formation and chromosome movement in mitosis. Cell *39*, 349–358.

Howell, B. J., McEwen, B. F., Canman, J. C., Hoffman, D. B., Farrar, E. M., Rieder, C. L., and Salmon, E. D. (2001). Cytoplasmic dynein/dynactin drives kinetochore protein transport to the spindle poles and has a role in mitotic spindle checkpoint inactivation. J. Cell Biol. *155*, 1159–1172.

Ikui, A. E., Furuya, K., Yanagida, M., and Matsumoto, T. (2002). Control of localization of a spindle checkpoint protein, Mad2, in fission yeast. J. Cell Sci. *115*, 1603–1610.

Kanbe, T., Hiraoka, Y., Tanaka, K., and Yanagida, M. (1990).The transition of cells of the fission yeast β-tubulin mutant nda3–311 as seen by freeze-substitution electron microscopy. Requirement of functional tubulin for spindle pole body duplication. J. Cell Sci. *96*, 275–282.

Kapoor, T. M., Lampson, M. A., Hergert, P., Cameron, L., Cimini, D., Salmon, E. D., McEwen, B. F., and Khodjakov, A. (2006). Chromosomes can congress to the metaphase plate before biorientation. Science *311*, 388–391.

Kremer, J. R., Mastronarde, D. N., and McIntosh, J. R. (1996). Computer visualization of three-dimensional image data using IMOD. J. Struct. Biol. *116*, 71–76.

Kuriyama, R., Kofron, M., Essner, R., Kato, T., Dragas-Granoic, S., Omoto, C. K., and Khodjakov, A. (1995). Characterization of a minus end-directed kinesin-like motor protein from cultured mammalian cells. J. Cell Biol. *129*, 1049–1059.

Maiato, H., DeLuca, J., Salmon, E. D., and Earnshaw, W. C. (2004). The dynamic kinetochore-microtubule interface. J. Cell Sci. *117*, 5461–5477.

Mao, Y., Desai, A., and Cleveland, D. W. (2005). Microtubule capture by CENP-E silences BubR1-dependent mitotic checkpoint signaling. J. Cell Biol. *170*, 873–880.

Mastronarde, D. N. (1997). Dual-axis tomography: an approach with alignment methods that preserve resolution. J. Struct. Biol. *120*, 343–352.

Mayer, C., Filopei, J., Batac, J., Alford, L., and Paluh, J. L. (2006). An extended anaphase signaling pathway for Mad2p includes microtubule organizing center proteins and multiple motor-dependent transitions. Cell Cycle *5*, 1456–1463.

Mazumdar, M., and Misteli, T. (2005). Chromokinesins: multitalented players in mitosis. Trends Cell Biol. *15*, 349–355.

McIntosh, J. R., Grishchuk, E. L., and West, R. R. (2002). Chromosome-microtubule interactions during mitosis. Annu. Rev. Cell Dev. Biol. *18*, 193–219.

Meluh, P. B., and Rose, M. D. (1990). KAR3, a kinesin-related gene required for yeast nuclear fusion. Cell *60*, 1029–1041.

Morales-Mulia, S., and Scholey, J. M. (2005). Spindle pole organization in *Drosophila* S2 cells by dynein, abnormal spindle protein (Asp), and KLP10A. Mol. Biol. Cell *16*, 3176–3186.

Moreno, S., Klar, A., and Nurse, P. (1991). Molecular genetic analysis of fission yeast *Schizosaccharomyces pombe.* Methods Enzymol. *194*, 795–823.

Nicklas, R. B. (1997). How cells get the right chromosomes. Science *275*, 632–637.

O'Toole, E. T., Winey, M., and McIntosh, J. R. (1999). High-voltage electron tomography of spindle pole bodies and early mitotic spindles in the yeast *Saccharomyces cerevisiae.* Mol. Biol. Cell *10*, 2017–2031.

Paluh, J. L., Nogales, E., Oakley, B. R., McDonald, K., Pidoux, A. L., and Cande, W. Z. (2000). A mutation in gamma-tubulin alters microtubule dynamics and organization and is synthetically lethal with the kinesin-like protein pkl1p. Mol. Biol. Cell *11*, 1225–1239.

Pidoux, A. L., LeDizet, M., and Cande, W. Z. (1996). Fission yeast pkl1 is a kinesin-related protein involved in mitotic spindle function. Mol. Biol. Cell *7*, 1639–1655.

Rieder, C. L., and Salmon, E. D. (1998). The vertebrate cell kinetochore and its roles during mitosis. Trends Cell Biol. *8*, 310–318.

Saitoh, S., Ishii, K., Kobayashi, Y., and Takahashi, K. (2005). Spindle checkpoint signaling requires the Mis6 kinetochore subcomplex, which interacts with Mad2 and mitotic spindles. Mol. Biol. Cell *16*(8), 3666–3677.

Savoian, M. S., Goldberg, M. L., and Rieder, C. L. (2000). The rate of poleward chromosome motion is attenuated in *Drosophila* zw10 and rod mutants. Nat. Cell Biol. *12*, 948–952.

Schaar, B. T., Chan, G. K., Maddox, P., Salmon, E. D., and Yen, T. J. (1997). CENP-E function at kinetochores is essential for chromosome alignment. J. Cell Biol. *139*, 1373–1382.

Schmidt, D. J., Rose, D. J., Saxton, W. M., and Strome, S. (2005). Functional analysis of cytoplasmic dynein heavy chain in *Caenorhabditis elegans* with fast-acting temperature-sensitive mutations. Mol. Biol. Cell *16*, 1200–1212.

Sharp, D. J., Rogers, G. C., and Scholey, J. M. (2000). Cytoplasmic dynein is required for poleward chromosome movement during mitosis in *Drosophila* embryos. Nat. Cell Biol. *2*, 922–930.

Tanaka, K., Mukae, N., Dewar, H., van Breugel, M., James, E. K., Prescott, A. R., Antony, C., and Tanaka, T. U. (2005a). Molecular mechanisms of kinetochore capture by spindle microtubules. Nature *434*, 987–994.

Tanaka, T. U., Stark, M.J.R., and Tanaka, K. (2005b). Kinetochore capture and bi-orientation on the mitotic spindle. Nat. Rev. Mol. Cell Biol. *6*, 929–942.

Troxell, C. L., Sweezy, M. A., West, R. R., Reed, K. D., Carson, B. D., Pidoux, A. L., Cande, W. Z., and McIntosh, J. R. (2001). pkl1(+)and klp2(+): two kinesins of the Kar3 subfamily in fission yeast perform different functions in both mitosis and meiosis. Mol. Biol. Cell *12*, 3476–3488.

Tytell, J. D., and Sorger, P. K. (2006). Analysis of kinesin motor function at budding yeast kinetochores. J. Cell Biol. *172*, 861–874.

Uzawa, S., Li, F., Jin, Y., McDonald, K. L., Braunfeld, M. B., Agard, D. A., and Cande, W. Z. (2004). Spindle pole body duplication in fission yeast occurs at the G1/S boundary but maturation is blocked until exit from S by an event downstream of *Cdc10*. Mol. Biol. Cell *15*, 5219–5230.

Walczak, C. E., Vernos, I., Mitchison, T. J., Karsenti, E., and Heald, R. (1998). A model for the proposed roles of different microtubule-based motor proteins in establishing spindle bipolarity. Curr. Biol. *8*, 903–913.

Yamamoto, A., West, R. R., McIntosh, J. R., and Hiraoka, Y. (1999). A cytoplasmic dynein heavy chain is required for oscillatory nuclear movement of meiotic prophase and efficient meiotic recombination in fission yeast. J. Cell Biol. *145*, 1233–1249.

Yamamoto, A., and Hiraoka, Y. (2003). Monopolar spindle attachment of sister chromatids is ensured by two distinct mechanisms at the first meiotic division in fission yeast. EMBO J. *22*, 2284–2296.

Zhu, C., Zhao, J., Bibikova, M., Leverson, J. D., Bossy-Wetzel, E., Fan, J.-B., Abraham, R. T., and Jiang, W. (2005). Functional analysis of human microtubule-based motor proteins, the kinesins and dyneins, in mitosis/cytokinesis using RNA interference. Mol. Biol. Cell *16*, 3187–3199.